

Introduction

Following earlier attempts by Weber cite: weber, Forward cite: forward and Weiss cite: weiss, several groups have been engaged in building detectors and observatories to study gravitational radiation from astrophysical sources. Among those which seem most likely to emit signals strong enough and often enough to trigger current detectors are inspiralling binary neutron stars from distances up to the Virgo cluster.

Detectors may be classified as either resonant mass or interferometric. We will be concerned with the latter only.

Interferometric detectors rely on detecting relative phase changes between a pair of mutually orthogonal light beams intersecting a pulse of gravitational radiation. Interference patterns jiggle because of momentary differences in the time-delay caused by metric perturbations by a pulse of a passing gravity wave.

Sensitivity Calculations

The interferometer arms are aligned along the x – and y – axes. The arms are of length L as measured in flat space. The gravitational wave described by a four-vector $k_\rho = (\omega, \mathbf{k})$, which is incident along the z – axis, perturbs the metric by a small amplitude. The background is a flat metric ($\eta_{\mu\nu}$); the perturbed metric is:

$$g_{\mu\nu} = \eta_{\mu\nu} + h_{\mu\nu} \quad \#$$

A null vector represents light in the interferometer. Because of the x – and y – alignment of the arms we need consider only the (11) and (22) components of the metric: the beam splitter and mirrors are in free fall.

$$\begin{aligned} ds^2 = 0 &= g_{\mu\nu} dx^\mu dx^\nu = (\eta_{\mu\nu} + h_{\mu\nu}) dx^\mu dx^\nu \quad \# \\ 0 &= -c^2 dt^2 + [1 + h_{11}(\omega t - \mathbf{k} \cdot \mathbf{x})] dx^2 \quad \# \end{aligned}$$

The gravity wave affects both time and space components. The coordinate length L is altered to proper length $L_x = L + \xi^1$ (Eq.(ref: h2)). Along the x – axis the round-trip light travel time is:

$$\tau_{rt} = \frac{2L_x}{c} + \frac{1}{2c} \int_0^{L_x} h_{11}(\omega t - \mathbf{k} \cdot \mathbf{x}) dx - \frac{1}{2c} \int_{L_x}^0 h_{11}(\omega t - \mathbf{k} \cdot \mathbf{x}) dx \quad \#$$

A similar integral appears for the y – axis with h_{22} substituted for h_{11} and the limit $L_y = L + \xi^2$. In the transverse traceless gauge we are working with $h = h_{11} = -h_{22}$; the arm lengths are affected in opposite directions. h is assumed to be constant over the range of the integral.

The integrals may be evaluated to obtain the difference in round-trip travel times between the x – and y – axes. The time difference is:

$$\Delta\tau_i = 2 \frac{\xi^1 - \xi^2}{c} + h(t) \frac{2L_i}{c} = h(t) \frac{2L_i}{c} + h(t) \frac{2L_i}{c} \leq 2h(t)\tau_i. \quad \#$$

where τ_i is the proper round-trip time for the i -th beam traversing the interferometer:

$$\tau_i = 2 \left[\frac{L_x + L_y}{c} \right] = \frac{2L_i}{c} \quad \#$$

obtained after substituting $h_{11} = -h_{22}$ in Eq.(ref: h2). For an explanation of the \leq condition in Eq.(ref: dtau) see section C.1 and Eq.(ref: phii). In the interferometer we will be describing, the

interference intensity is recorded in discrete samples. Each sample is τ_i in duration. This method of sampling requires identification of the i -th beam.

Two aspects of this result (Eq.(ref: dtau)) are noticeable (i) there is a time difference $\Delta\tau_i$ even though h is constant in the interval 0 to L_x and (ii) even when the lengths of the arms are nominally equal. The metric perturbs both clock rates and lengths. Furthermore, in a region where space-time is flat i.e., $h = 0$, $\Delta\tau_i = 0$. These properties are a consequence of the intrinsic curvature in the geometry of the gravity wave. The incident gravity wave has intrinsic curvature (non-zero Riemann tensor), recall that $h_{11} = -h_{22}$, implying a wave-front surface that is saddle-like (Fig. 1).

The time delay can be related to the phase difference in monochromatic light beams of wavelength λ :

$$\Delta\phi_i \leq 2h\tau_i \frac{2\pi c}{\lambda} \quad \#$$

In the design we are describing the light beams which traverse the interferometer are sampled after each reflection, so $\Delta\phi_i$ is the phase difference acquired by the i -th light beam in the time the beam is under the influence of the external metric perturbation $h_{\mu\nu}$: $\Delta\phi_i \propto h$ also $\Delta\phi_i \propto \tau_i$ i.e., the exposure time. Later we will extend the exposure time to the duration of the gravity wave pulse. The angle $\Delta\phi_i$ may be interpreted as the excess angle acquired by a null-vector (light beam) parallel transported simultaneously along two closed loops (x – and y –axes), in a curved metric. These observations will be used later.

The interferometer has an input and an output port. The laser power at these ports is P_{in} and P_{out} respectively. The minimum sensitivity depends, among other factors, on the fluctuation of the laser intensity. The average photon flux is:

$$\bar{n} = \frac{P_{out}}{\hbar \frac{2\pi c}{\lambda}} = \frac{P_{out}}{2\pi\hbar} \frac{\lambda}{c} \text{ sec}^{-1} \quad \#$$

Under operating conditions where the mean power at the output port of the interferometer averaged over one circuit time interval is half the mean power at the input port, i.e.,

$$P_{out} = \frac{1}{2}P_{in} \quad \#$$

The equivalent minimum detectable metric perturbation for a laser with wavelength λ is

cite: saulson:

$$h_i \geq \frac{1}{2} 5.2 \times 10^{-23} \text{ Hz}^{-1/2} \left(\frac{1000 \text{ km}}{L_i} \right) \sqrt{\frac{\lambda}{0.545 \mu\text{m}}} \sqrt{\frac{1 \text{ watt}}{P_{in}}} \quad \#$$

again for the i -th sample. The $\geq (1/2)$ factor is a correction. This expression assumes that shot noise is dominant; Brownian noise and radiation pressure noise are negligible; generally true for the example under consideration (see C.1).

Detection Scheme

Over-sampled detector

Equation (ref: hmin) suggests a long interferometer arm to reduce the sensitivity to values expected as a result for example, of infalling binary stars from as far as the Virgo cluster. The expected signal is a pulse of duration $\tau \sim 10 \text{ ms}$ of $h \sim 10^{-21}$ centered at a frequency of $\sim 800 \text{ Hz}$.

However, there is another approach which is appealing because of its simplicity. It takes advantage of sampling theory. Generally, the minimum sampling frequency, called the Nyquist frequency, is twice the bandwidth of the signal to be sampled. For example, a signal with a

bandwidth of 100Hz need be sampled every 200Hz, under ideal conditions, to be reproduced flawlessly. Practical considerations dictate the technique of "over-sampling", that is, sampling at rates which are integer multiples of the Nyquist frequency. The original signal is reproduced from sampled segments.

Since the sampling interval is short, one needs to revise the sensitivity calculations. For instance a shorter sampling period will be accompanied by an increase in the photon noise in each sample. Countering this increase in noise is the increase in the number of samples.

Light from a laser enters a Michelson interferometer. It passes through a beam-splitter, reflects off two mirrors onto a photodiode where the interference intensity is recorded (Fig. 2). Let τ_i be the travel time for the i -th beam. The photodiode output is averaged over an interval τ_i . The averaged intensity is that of the i -th sample.

The over-sampling frequency is $f_S \sim GHz$ for the example we will describe, compared with the signal bandwidth $f_B = 800Hz$. Thus the over-sampling frequency is 10^6 times the Nyquist frequency.

We give an example of what can be achieved in an $L_i = 10cm$ Michelson interferometer. Using a 1 watt light source of wavelength $0.545\mu m$, and sampling every nanosecond ($\tau_i = (2/3) \times 10^{-9} sec$), the minimum sensitivity for the i -th sample of the expected gravity wave pulse, is:

$$h_i = 5.2 \times 10^{-23} \left(\frac{1000km}{L_i} \right) \sqrt{\frac{1}{\tau_i}} = 5.2 \times 10^{-23} \left(\frac{1000km}{L_i} \right) \sqrt{\frac{c}{2L_i}} \quad \#$$

This expression is obtained by imposing the condition that the signal to noise ratio is unity. The maximum number of samples is the maximum number of round-trips limited by the pulse duration:

$$N = \frac{10^{-2} \text{ secs}}{\tau_i} = \frac{10^{-2}c}{2L_i} = 1.5 \times 10^7 \quad \#$$

The light beam acquires an excess angle $\Delta\phi_i$ at the end of *each* round-trip. Since the duration of the pulse is expected to be 10^{-2} secs, one may collect as many as 1.5×10^7 discrete samples or equivalently a total phase change of

$$\Delta\phi = \sum_{i=1}^N \Delta\phi_i = N\Delta\phi_i = 1.5 \times 10^7 \Delta\phi_i$$

this follows from the earlier observation that $\Delta\phi_i \propto \tau_i$ i.e., the phase accumulates with τ . In fact the intrinsic curvature of the gravity field requires this. It is worth emphasizing that the accumulated phase makes no distinction whether it was acquired in one round-trip or several independent round-trips of the same total duration; what matters is the total sampling interval or equivalently, the integration bandwidth (property of linear systems).

In one pass the sensitivity is:

$$h_i = 5.2 \times 10^{-23} \left(\frac{1000km}{L_i} \right) \sqrt{\frac{1}{\tau_i}} = 5.2 \times 10^{-23} \left(\frac{1000km}{L_i} \right) \sqrt{\frac{c}{2L_i}}$$

As the signal strength grows with each reflection, the noise, since it adds in quadrature, decreases as the square root: for N passes the sensitivity is:

$$h = 5.2 \times 10^{-23} \left(\frac{1000 \text{km}}{NL_i} \right) \sqrt{\frac{c}{2L_i}} \sqrt{\frac{1}{N}} \quad \#$$

$$h = 5.2 \times 10^{-23} \left(\frac{1000 \text{km}}{L_i} \right) \frac{2L_i}{10^{-2}c} \sqrt{\frac{c}{2L_i}} \frac{2L_i}{10^{-2}c} \quad \#$$

$$h = 3.5 \times 10^{-22} \quad \#$$

a result which depends only on the pulse duration but remarkably is independent of the sampling interval τ_i , and necessarily, the length L_i . The equivalent length of the interferometer is 1500km, half the distance a light beam travels during the 10m sec gravitational wave pulse; this is also the optimum length. The sensitivity is sufficient to detect putative events from distances up to the Virgo cluster.

Sampling permits extraction of signals even when the light spends one or more gravitational wave periods in the interferometer.

Unlike a Fabry-Perot cavity or a Herriot delay line where the light beam is recorded after it undergoes multiple reflections in a cavity, we note that the light beam is averaged, and recorded at the end of *each round-trip*. The sampled data stream is processed in accordance with algorithms used for over-sampled detection. The proposed design differs in this aspect from folded interferometers.

Proposed Design

Once we realize that the sensitivity is independent of L , the interferometer arms are chosen for convenience to be 10cm long; the design options also allow some flexibility. For one; a small interferometer is easier to build, easier to control the environment (temperature, pressure, isolation from external noise etc.). Sampling the signal at the end of every round-trip prevents the accumulation of excess phase by using the beams only once.

Mechanical stability is facilitated by mounting all the components on a 15cm diameter, 2cm thick sapphire disk. Sapphire is a suitable material because of its low thermal expansion coefficient ($\alpha \sim 10^{-6}/\text{C}^\circ$), excellent thermal conductivity (0.4watts/cmK $^\circ$), low mechanical dissipation ($Q \approx 10^9$, reduces Brownian noise), stiff Young's modulus (~GPa) and a high speed of sound (10^4m/s) cite: sapphire, so a high fundamental vibration frequency which facilitates isolation from external vibrations.

Noise from Brownian motion and radiation pressure

We can estimate the Brownian noise contribution. The mirrors, which. need be no more than 5mm in diameter, and in order to maintain the high fundamental frequency, may be sculpted directly into the sapphire disk. For reasons why the mirrors need not be "free" see later. The entire platform vibrates due to thermal excitation. Far below the fundamental resonance at ω_0 its amplitude excursion is:

$$x_{rms}^B = \sqrt{\frac{4k_B T Q^{-1}}{\omega m \omega_0^2}} = 2.1 \times 10^{-18} \text{m} / \sqrt{\text{Hz}} \quad \#$$

for $T = 300\text{K}$, $Q \sim 10^6$, $m = 1\text{kg}$, $\omega_0 \approx 2\pi \times 10^4 \text{Hz}$ (for its chosen value, see C.1). After N discrete samples each of interval τ_i , the average excursion is

$$x_{rms}^B = \sqrt{\frac{4k_B T Q^{-1}}{\omega m \omega_0^2}} \sqrt{\frac{1}{\tau_i}} \sqrt{\frac{1}{N}} = \sqrt{\frac{4k_B T Q^{-1}}{\omega m \omega_0^2}} \sqrt{\frac{c}{2L_i}} \sqrt{\frac{2L_i}{10^{-2}c}} = 2 \times 10^{-17} \text{m} \quad \#$$

x_{rms}^B depends on the total sampling interval, independent of the number of samples or the individual sampling interval.

There is a time jitter due to Brownian motion. The elapsed time of $10ms$ incurs an uncertainty of $\pm x_{rms}^B/c$. There is a factor of 2 because it takes two traverses to collect each sample. The relative time uncertainty is then:

$$\langle \sigma^B \rangle = \frac{2 \times 10^{-17} m}{3 \times 10^8 m/sec} \frac{2}{10^{-2} sec} = 1.3 \times 10^{-23}$$

We propose using a laser of $P_{in} = 1\text{watt}$ and $\lambda = 0.545\mu\text{m}$. Radiation pressure will induce random vibrations in the mirrors. The appropriate expression to use is

$$x_{rms}^R = \frac{1}{m\omega^2} \sqrt{\frac{4\pi\hbar P_{in}}{c\lambda}} \sqrt{\frac{1}{\tau_i}} \sqrt{\frac{1}{N}} = \frac{2.89 \times 10^{-17} m}{\omega^2} \quad \#$$

under the same conditions. Again the relative time uncertainty is:

$$\langle \sigma^R \rangle = \frac{2.89 \times 10^{-17} m}{3 \times 10^8 m/sec} \frac{1}{\omega^2} \frac{2}{10^{-2} sec} = \frac{1.9 \times 10^{-23}}{\omega^2}$$

These should be compared with the photon noise strain figure for $10ms$ averaging interval Eq.(ref: hstr):

$$h = 3.5 \times 10^{-22} \quad \#$$

Noise due to radiation pressure Eq.(ref: rad) dominates when $\omega \leq 0.28$ or 0.05Hz . The detector is shot noise limited for frequencies above $\approx 10^{-1}\text{Hz}$. Noise from radiation pressure becomes significant only at low frequencies. Brownian noise can be ignored.

It is worth repeating that the light beams reflect off each mirror only once, then they strike the photo-diode and are removed from the interferometer. Light from single reflections is corrupted by fluctuations in the mirror position due to radiation pressure and/or shot noise. Because each reflection is independent, the noise contributions are also independent. They add in quadrature. By contrast the situation in folded interferometers which utilize multiple reflections, is different because mirror noise fluctuations accumulate with each reflection, in practice limiting the number of folded beams cite: saulson.

Measurement Method

The photodiode detects interference fringes, actually a circular region which may be all shades from completely dark to completely bright. The photodiode output is sampled every nanosecond. To make data handling manageable, the photodiode output is fed first into an analogue integrator with a time constant which is a small fraction of the expected (reciprocal) signal frequency. For example a $10\mu\text{sec}$ time constant is sufficient for 125 samples of an 800Hz signal or 1000 samples of a 100Hz signal. Following the integrator the averaged signal is sent to a 16-bit analogue to digital converter and from there onto a library for comparison against different signal templates.

Referring to the earlier mention of a mode of operation Eq.(ref: ops), it turns out that refinements are needed to operate the interferometer as a null detector. Pockels cells need to be inserted to provide phase modulation. The interferometer operation point is moved to a dark fringe cite: weiss. Because of the stiff mounting of the mirrors, it may be possible to maintain the dark fringe condition by further slow modulation of the Pockels cells.

Response of interferometer and mirror mount

The interferometer responds to the incident gravity wave. The interferometer is a rigid platform. It is accelerating upwards to counter Earth's gravity. Acceleration, in principle, affects both mirror spacing and time delay. These effects are taken care of by equations of special relativity. For a detailed discussion and experimental confirmation see

cite: MTW, cite: hay. For a system accelerating $@g \approx 10m/sec^2$, times and lengths will change according to cite: martin:

$$t = t_0 + (c/g) \sinh(g\tau/c) \text{ and } x = x_0 + (c^2/g)[\cosh(g\tau/c) - 1]$$

For measurement intervals $\tau \ll 1$ secs there is negligible change in either t or x . Acceleration is not an issue, the system is in practice, inertial.

What is the effect of the rigid platform? The time delay Eq.(ref: dtau) is the sum of contributions from time and space components.

Since the phase of a plane wave is an invariant quantity i.e., $\phi = \omega t - \mathbf{k} \cdot \mathbf{x} = \omega' t' - \mathbf{k}' \cdot \mathbf{x}'$, a change in phase requires a change in both the time and space components. A quick way to see why there are two independent sources of the phase Eq.(ref: dphi) is to follow the world lines of the light rays emerging from the beam-splitter as they reflect off the two mirrors (Fig. 3). The mirrors are shown in two configurations: (i) in free fall and (ii) attached rigidly to the interferometer. In the frame of the platform the mirrors are displaced in the same sense as in the freely falling case, but less so in the case of rigid mounts. In either case, whether in free fall or rigidly attached, there is a path difference Eq.(ref: h2). Time and space components are affected independently. A quantitative discussion follows.

In the initial calculation the beam-splitter and mirrors were treated as test masses in free fall. Thus mirrors and beam-splitter move along individual geodesics. Following this reasoning it is generally believed that the mirrors must be mounted on "soft" springs such as long-period pendulums. The calculations go like this: $\Delta\tau$ measures the difference in light travel times between the beam splitter and mirrors in free fall. However, measurements are made using rigid rulers in a non-inertial laboratory. In this laboratory one of the mirrors, of mass m is instantaneously at rest at a coordinate x^j with origin at the beam-splitter. The waves produce small oscillations of the test mass of amplitude ξ^j . The wave is so weak that $\xi^j \ll x^j$ thus x^k is essentially constant. Integration gives cite: thorne

$$\xi^j = \frac{1}{2} h_{jk} x^k \quad \#$$

When h_{jk} is time-varying as is the case for gravity waves, one can calculate the response as follows: Consider the mirrors as test masses connected through a spring of force constant k_a^μ with damping constant b_a^μ . The interferometer is in free fall. We may use geodesic coordinates where the Christoffel symbols are made zero cite: martin on all points on the geodesic. The geodesic is the world line of the beam-splitter. The time coordinate is along the instantaneous tangent to the world line of the beam-splitter. There is an orthogonal comoving coordinate with the mirror lying on the x -axis. The quantities ($h_a^\mu = h$, $k_a^\mu = k$, $b_a^\mu = b$) have only one component. The equation of motion which describes the mirror of mass m that has an instantaneous position x^1 is cite: weber:

$$\frac{d^2 \xi^1}{dt^2} + \frac{b}{m} \frac{d\xi^1}{dt} + \omega_0^2 \xi^1 = -R_{1010}^{GW} x^1 = \frac{1}{2} \frac{\partial^2 \tilde{h}_{11}}{\partial t^2} x^1 = -\frac{1}{2} \omega^2 x^1 \tilde{h}_{11} \quad \#$$

where $\tilde{h}_{jk} = h_{jk} \sin \omega t$ and $\omega_0 \equiv k/m$. We solve this equation for $Q \equiv \omega_0 m/b \gg 1$ or $(b/m) \ll 1$. With $x^1 = L$ the solution is:

$$\frac{\xi^1}{L} = \frac{1}{2} h_{11} \omega^2 \frac{\sin \omega t}{\omega^2 - \omega_0^2} \quad \#$$

For the mirror on the y -axis there is a similar equation:

$$\frac{d^2\xi^2}{dt^2} + \frac{b}{m} \frac{d\xi^2}{dt} + \omega_0^2 \xi^2 = \frac{1}{2} \frac{\partial^2 \tilde{h}_{22}}{\partial t^2} x^2 = -\frac{1}{2} \omega^2 \tilde{h}_{22} x^2 \quad \#$$

Under the same conditions the solution of this equation is:

$$\frac{\xi^2}{L} = \frac{1}{2} h_{22} \omega^2 \frac{\sin \omega t}{\omega^2 - \omega_0^2} \quad \#$$

where $x^2 = L$. The differential strain, with $h \equiv h_{11} = -h_{22}$, is

$$\frac{\xi^1 - \xi^2}{L} = h \sin \omega t \frac{\omega^2}{\omega^2 - \omega_0^2} \equiv h(t) \frac{\omega^2}{\omega^2 - \omega_0^2} \quad \#$$

For $\omega_0 \ll \omega$, one recovers the expression for freely falling mirrors Eq.(ref: h2), the factor 1/2 is missing because there are two mirrors. Thus choosing a "soft" spring, such as a pendulum of length l and spring constant $k = mg/l$, emulates a free mass suspension, which satisfies the condition $\omega_0 \ll \omega$. This is the preferred design in the LIGO detector.

Eq.(ref: h2) says that the elastic properties of the mirror suspension, whether "soft" or rigid, are modified by the incident gravity wave. For the example under study the restoring force goes from $kx^1 \rightarrow kx^1 + k\xi^1 = kx^1(1 + \frac{1}{2}h) \equiv k'x^1$ and $kx^2 \rightarrow kx^2(1 - \frac{1}{2}h) \equiv k''x^2$. Along the x -axis the elastic constant increases from $k \rightarrow k'$ and decreases as $k \rightarrow k''$ along the y -axis. The position of the mirror does not change; the ruler itself expands or contracts by ξ^j in phase with the gravity wave.

The gravity wave has two independent effects; (i) it alters clock rates (ii) it changes lengths. Just as the gravity wave changes the time delay from $\tau_i \rightarrow \tau_i + h\tau_i$, so does it alter the length $2L \rightarrow 2L + h2L$ (Eq.(ref: dtau)). Again since phase is a scalar, both contributions are simultaneous and independent. They are also in the same sense as they must be for the ratio to be c , the speed of light measured by local observers.

Figure 3 shows the effect of a gravity wave on world lines of two types of mirrors, freely falling and rigid. In frame of the platform the limits of the integrals in Eq.(ref: taurt) are changed from 0 to L to 0 to $L + \xi^1$ and 0 to $L + \xi^2$ along the x - and y -axes respectively.

Time and space contributions add in phase because the speed of sound in sapphire is $\approx 10^4$ m/sec; the mirrors respond almost instantaneously i.e., within $0.10m/10^4m/s = 10\mu$ sec, much less than the period 1/800 sec. The total phase difference is the sum of the time and space contributions.

$$\Delta\phi_i = \tau_i h \frac{2\pi c}{\lambda} + 2 \frac{\xi^1 - \xi^2}{c} \frac{2\pi c}{\lambda} = \tau_i h \frac{2\pi c}{\lambda} \left(1 + 2 \frac{\xi^1 - \xi^2}{c} \frac{c}{2L_i} \right) = \tau_i h \frac{2\pi c}{\lambda} \left(1 + \frac{\omega^2}{\omega^2 - \omega_0^2} \right) \quad \#$$

For a stiff mount, which is more practical given the problems of vibration isolation, one may choose a high fundamental mode. For example if $\omega_0 = 2\pi \times 10^4$, and for a maximum driving frequency $\omega = 2\pi \times 800$, $(\xi^1 - \xi^2)/L \geq -0.006h$ rather than h for soft mounts; the phase difference is almost entirely due to time component of the metric perturbation. There is an acceptable reduction in strain amplitude (by a factor of 1/2) in exchange for ease in vibration isolation.

As mirror mounts are a major obstacle in interferometric detectors, being able to mount them in rigid platforms alleviates many problems, including noise due to Brownian motion.

The small size of the interferometer (diameter 15cm.) facilitates operation in a vacuum environment (10^{-7} T is sufficient for $h = 3.5 \times 10^{-22}$); it also opens up several schemes to isolate it from seismic vibrations which is a major source of noise at low frequencies. Isolation from ground vibrations is made easier because the design fundamental mode is $\omega_0 = 2\pi \times 10^4$.

This is one great advantage in using rigidly mounted mirrors and a high-Q platform.

The interferometer needs a laser source stabilized against both intensity and frequency drifts. Use of sapphire also minimizes platform distortions due to temperature inhomogeneities. Instruments will be needed to monitor and control the temperature.

The scheme described here can be extended to a three-axis detector, which may be replicated and installed as an antenna array on several optimal locations on Earth, sent into orbit, even mounted on the Moon.

Conclusion *We have shown how use of signal processing techniques may allow a table-top 10cm Michelson interferometer sufficient sensitivity to detect gravitational waves from infalling binary neutron stars from as far as the Virgo cluster.*

We acknowledge with gratitude an anonymous referee for planting the seed of an idea, and M. Bocko for technical advice.

weber J. Weber, *General Relativity and Gravitational Waves*, (Interscience Publishers, New York, 1961)

forward G.E. Moss, L.R. Miller, R.L. Forward, *Appl. Optics*, **10**, 2495 (1971), R.L. Forward, *Phys. Rev. D* **17**, 379 (1978)

weiss R. Weiss, *MIT Quart. Prog. Rep.* **105**, 54 (1972)

saulson P.R. Saulson, *Fundamentals of Interferometric Gravitational Wave Detectors*, (World Scientific, Singapore, 1994)

LIGO <http://www.ligo.caltech.edu>

sapphire <http://www.saphikon.com>

thorne K. S. Thorne in *300 Years of Gravitation*, Eds. S. Hawking and W. Israel, (Cambridge University Press, 1987)

martin J.L. Martin, *General Relativity*, (Prentice Hall, 1988, 1996)

MTW C.W. Misner, K.S. Thorne and J.A. Wheeler, *Gravitation*, p. 63 (W.H. Freeman, San Francisco, 1973)

hay H.J. Hay, J.P. Schiffer and P.A. Egelstaff, *Phys. Rev. Lett.* **4**, 165 (1960), W. Kündig, *Phys. Rev.* **129**, 2371 (1963), D.C. Champeney, G. R. Isaak and A.M. Khan, *Phys. Lett.* **7**, 241 (1963), G.R. Isaak, *Phys. Bull.* **21**, 255 (1970). There was an experiment performed where relativistic muons were slammed into a beam dump. The enormous deceleration was meant to simulate a strong gravity field which would presumably slow down the muon decay rate. No general relativistic effects were observed, only the usual time dilation expected from special relativity; confirming that acceleration is not a substitute for gravity. Unfortunately I haven't been able to find the reference.

Figures

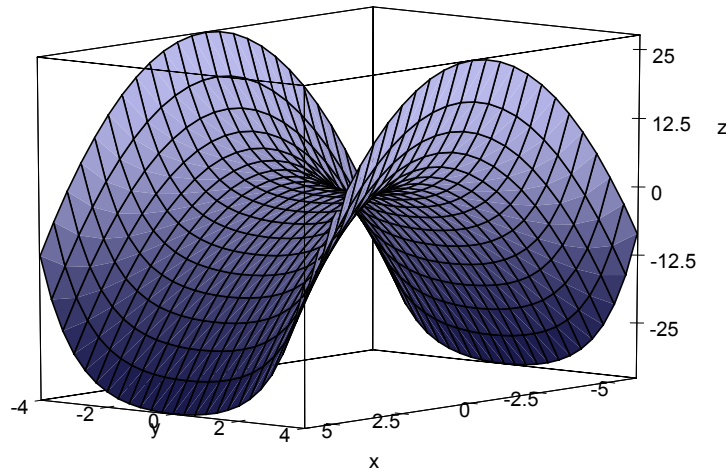
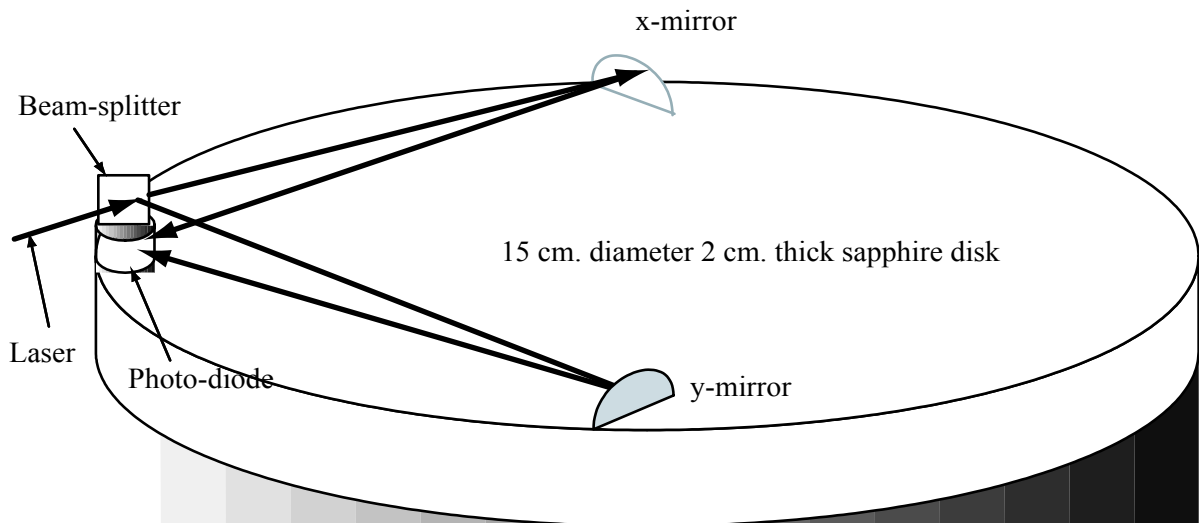


Figure 1. Surface of gravity wave-front. Shown is the field amplitude h_{uv} along the z-axis: at this instant h_{11} is along the x-axis and h_{22} is along the y-axis. The surface has intrinsic curvature. An excess phase appears in a null vector parallel transported in a circuit on this surface. $\Delta\phi_i$ is the difference in excess phase between a circuit along the x – and y – axes.



Sampled gravity wave interferometer

Figure 2. Schematic arrangement of interferometer components. Coherent beams reflect off the x – and y – mirrors, when they strike the photo-diode they exit the interferometer. Output is sampled in discrete intervals: the intensity pattern is reconstructed using sampling algorithms. Each sample is independent, there is no multiple reflection.

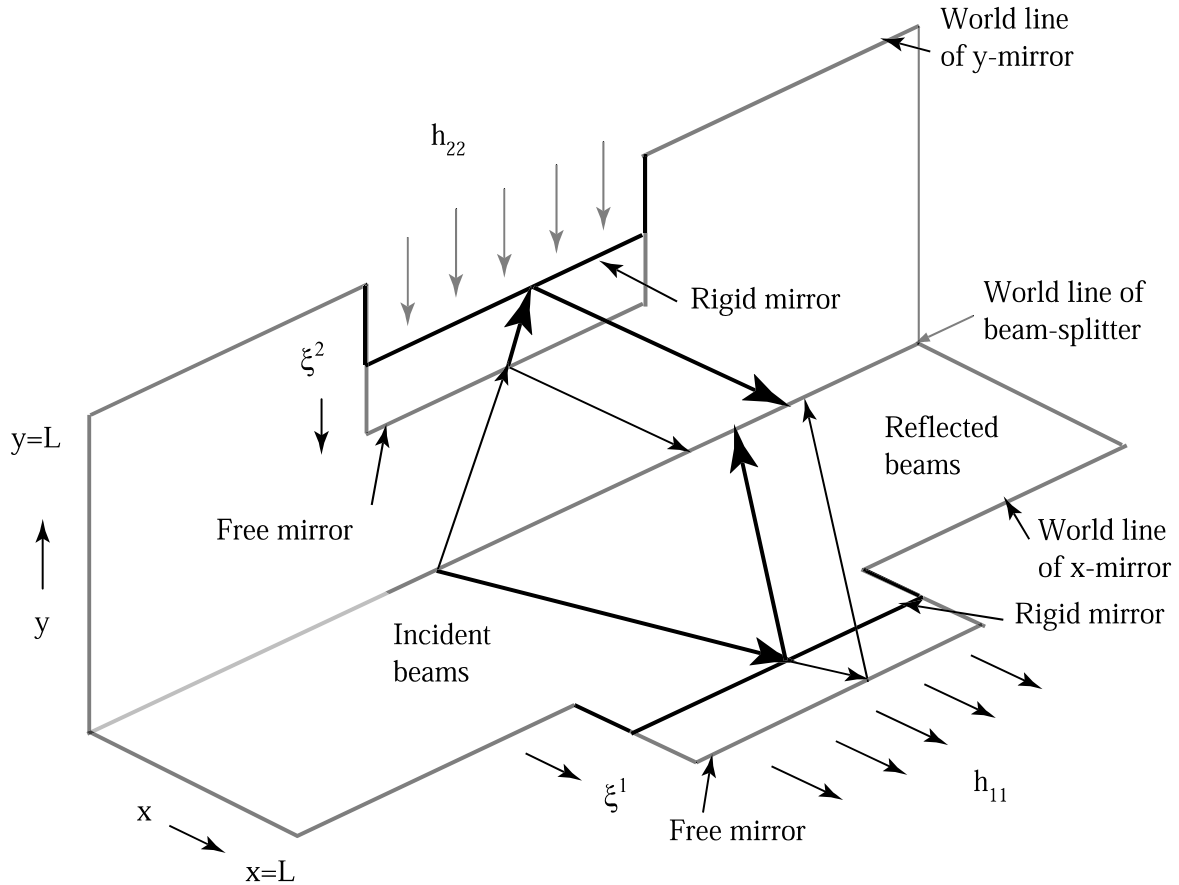


Figure 3. World lines of rays and interferometer components. Two mirror mounts, free in light and rigid in heavy lines, are shown under the influence of a gravity wave of amplitude $h_{\mu\nu}$. Although the surfaces are shown as planes they are saddle-shaped as in figure 1. The reflection points depend on the type of mirror mount, and so does the excess phase.